# Superbunching from Coherently Driven Atoms in a Waveguide



Citation for the original published paper (version of record):
Zeidan, Z., Karmstrand, T., Khanahmadi, M. et al (2026). Superbunching from Coherently Driven Atoms in a Waveguide. Physical Review Letters, 136(25). http://dx.doi.org/10.1103/6fcg-2zns

# Superbunching from Coherently Driven Atoms in a Waveguide

Zeidan Zeidan,[1,*] Therese Karmstrand,[1,2] Maryam Khanahmadi,[1] and Göran Johansson[1]
[1]*Department of Microtechnology and Nanoscience (MC2), Chalmers University of Technology, 41296 Gothenburg, Sweden*
[2]*Center for Quantum Computing, RIKEN, Wako-shi, Saitama 351-0198, Japan*

(Received 13 June 2025; revised 19 November 2025; accepted 27 May 2026; published 26 June 2026)

We investigate the scattered field from $N$ identical two-level atoms resonantly driven by a weak coherent field in a one-dimensional waveguide. For atoms separated by the drive wavelength, increasing the number of atoms suppresses transmission while enhancing photon bunching. Transmission becomes a superbunched $(N+1)$-photon scattering process that is predominantly incoherent. Remarkably, we find that transmission occurs through a process where all $N$ atoms are excited, enabling novel heralded multiphoton state generation with applications in long-distance entanglement and quantum metrology.

DOI: 10.1103/6fcg-2zns

*Introduction*—Nonlinear light-matter interactions have been studied for decades, leading to the discovery of various quantum phenomena, including nonclassical light state generation [1,2], antibunching [2,3], and superradiance [2,4–6]. Multiphoton states, in particular, enable applications in quantum metrology [7–9], entanglement generation for quantum communication [10,11], and quantum lithography [12,13].

Waveguide quantum electrodynamics (wQED) has shown to be a promising platform for light-matter interactions due to the strong coupling between atoms and propagating electromagnetic fields. Experimentally, wQED has been demonstrated on various platforms [2,14], including cold atoms coupled to nanofibers or photonic crystals [6,15–22], quantum dots in photonic crystals [23], and superconducting circuits [24–37]. While previous experimental work has focused on either one or two atoms or ensembles of hundreds to thousands of atoms, recent advances in atom-photon coupling efficiency, deterministic atom placement, and independent control have now made the previously inaccessible regime of a few to tens of atoms experimentally realizable across multiple platforms [38–48].

It is well established that an atom in a waveguide almost perfectly reflects a weak resonant drive and that the transmitted field is strongly bunched [14,24,26,27,29,31,49–53]. As noted in [53], the bunching occurs, somewhat counterintuitively, because a transmission event predominantly heralds the excitation of the atom, which then spontaneously emits a second photon. Given recent experimental progress, it is now timely to explore bunching in the few-atom regime.

In this Letter, we study the scattering of a resonant coherent state by $N$ atoms in a waveguide. When driving weakly, increasing the number of atoms progressively suppresses the transmission. We demonstrate that this is connected to a strongly enhanced bunching in the transmitted field. By considering atoms separated by the drive wavelength, we derive exact analytical expressions describing the scattering dynamics. We find that transmission in the weak-drive regime is a superbunched $(N+1)$-photon scattering process that is predominantly incoherent, with no phase relation to the drive. Remarkably, we analytically find that this transmission is possible only through a process where all $N$ atoms are collectively excited. Thus, the first detection of a transmitted photon in a bunch heralds the atomic system most likely in a fully excited state. Surprisingly, this collective excitation of all $N$ atoms emerges despite the weak driving strength. We verify our analytical findings with numerical simulations. Naturally, this simple setup enables a novel route to heralded multiphoton state generation with applications in entanglement distribution and quantum metrology.

*Model*—We consider $N$ identical atoms spaced one drive wavelength apart in a one-dimensional waveguide. The atoms are modeled as two-level systems with resonance frequency $\omega$ and are symmetrically coupled to the waveguide into which they decay through spontaneous emission with the rate $\gamma$ to the left- and right-propagating fields (see Fig. 1). Neglecting the time delay between the closely spaced atoms, the master equation for the density matrix $\rho$ of the atomic system, collectively and coherently driven with Rabi frequency $\Omega$, is

$$\dot{\rho} = -i\frac{\Omega}{2}[S_+ + S_-, \rho] + \mathcal{D}(a^R_{\mathrm{out}})\rho + \mathcal{D}(a^L_{\mathrm{out}})\rho, \quad (1)$$

*Contact author: zeidan.zeidan@chalmers.se

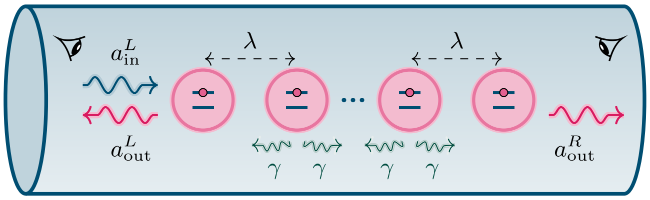


FIG. 1. $N$ identical atoms, modeled as two-level systems, coupled to a waveguide. The atoms are spaced apart by wavelength distance $\lambda$ and decay to the left- and right-propagating fields with spontaneous emission rate $\gamma$. The operator $a^L_{\rm in}$ refers to the annihilation operator of the incoming coherent drive from the left, and $a^{R/L}_{\rm out}$ is the operator of the outgoing field propagating toward the right or left. The eyes in the two corners represent photon detectors.

where $\hbar = 1$, $\mathcal{D}(L)\rho = L\rho L^\dagger - \frac{1}{2}\{L^\dagger L, \rho\}$ is the Lindblad dissipator, $S_\pm = \sum_{i=1}^N S^i_\pm$ are the collective atomic dipole operators, and $a^{R/L}_{\rm out}$ is the annihilation operator of the outgoing field propagating toward the right or left. The outgoing field operators are related to the annihilation operators of the incoming field from the right or left, $a^{R/L}_{\rm in}$, through the input-output relations $a^L_{\rm out} = a^R_{\rm in} + \sqrt{\gamma}S_-$ and $a^R_{\rm out} = a^L_{\rm in} + \sqrt{\gamma}S_-$ [28,54]. We consider an incoming coherent drive from the left with rate amplitude $\alpha = i\Omega/\sqrt{\gamma}$ and vacuum incoming from the right. Henceforth, we refer to photons from the coherent drive as input photons and to the right- and left-propagating output fields as transmitted and reflected photons, respectively. When individual atomic relaxation into nonwaveguide modes and time delays are negligible, an atomic system initialized in the ground state evolves within the symmetric $(N+1)$-dimensional Dicke subspace [4]. In the Hilbert space of the atomic system, the input-output relations then become $a^L_{\rm out} = \sqrt{\gamma}S_-$ and $a^R_{\rm out} = \alpha I_{N+1} + \sqrt{\gamma}S_-$, where $I_{N+1}$ is the identity operator. Using the input-output relations, we can rewrite Eq. (1) as $\dot{\rho} = 2\mathcal{D}(a^R_{\rm out})\rho$, to immediately obtain the steady-state solution [57–62]:

$$\rho = \frac{(a^{R\dagger}_{\rm out}a^R_{\rm out})^{-1}}{\mathrm{Tr}(a^{R\dagger}_{\rm out}a^R_{\rm out})^{-1}} = \frac{1}{D}\sum_{m,n=0}^{N}\left(\frac{S_-}{g^*}\right)^m\left(\frac{S_+}{g}\right)^n, \quad (2)$$

where the normalized drive amplitude $g = \alpha/\sqrt{\gamma} = i\Omega/\gamma$ and the normalization constant $D = \sum_{r=0}^N \binom{N+r+1}{2r+1} \times (r!)^2|g|^{-2r}$. Using the steady-state solution from Eq. (2), we now calculate the scattered photon rates, providing initial insight into the system's dynamics and photon bunching behavior.

*Scattered field*—The average photon rate in the reflected and transmitted directions is given by $\bar{n}_{\rm ref} = \langle a^{L\dagger}_{\rm out}a^L_{\rm out}\rangle$ and $\bar{n}_{\rm trans} = \langle a^{R\dagger}_{\rm out}a^R_{\rm out}\rangle$, respectively. The scattered photon rate comprises phase-coherent components $\bar{n}_{\rm ref,coh} = |\langle a^L_{\rm out}\rangle|^2$ and $\bar{n}_{\rm trans,coh} = |\langle a^R_{\rm out}\rangle|^2$, with the remaining phase-incoherent components given by $\bar{n}_{\rm ref/trans,inc} = \bar{n}_{\rm ref/trans} - \bar{n}_{\rm ref/trans,coh}$. The scattered phase-incoherent photons, attributed to spontaneous emission, are equal in the reflected and transmitted directions, $\bar{n}_{\rm ref,inc} = \bar{n}_{\rm trans,inc}$, due to the symmetry of emission into the waveguide. When weakly driven, $|g| \ll 1$, the atoms collectively oscillate coherently with a phase opposite to the input drive, leading to near-perfect reflection and effectively canceling the transmitted field [54], as in the single-atom case [14,24,26,27,29,31,49–53]. Notably, in this regime, the transmission is predominantly incoherent and is given by [54]

$$\bar{n}_{\rm trans} \approx \bar{n}_{\rm trans,inc} = \gamma|g|^{2(N+1)}\frac{N+1}{(N!)^2} + \mathcal{O}(|g|^{2(N+2)}), \quad (3)$$

which is proportional to the incoming rate of $(N+1)$-photon states from the Poissonian drive. The scaling in Eq. (3) reveals that transmission requires driving the atomic system with sufficient photons to excite all $N$ atoms. This behavior can be understood through two perspectives: (i) $N$ atoms can coherently reflect Fock states of up to $N$ photons, while states with $N+1$ or more photons enable incoherent transmission. (ii) Although the average drive amplitude is in the linear regime, amplitude fluctuations occasionally probe the atomic nonlinearity.

Moreover, in the weak-drive regime, the probability density for simultaneous detection of $n$ transmitted photons is proportional to the zero-time $n$ th-order correlation function [54,63]:

$$G^{(n)}_{\rm trans}(0) = \begin{cases} \gamma^n|g|^{2(N+1)}\binom{N+n}{2n-1}\left[\frac{(n-1)!}{N!}\right]^2 & \text{if } n \le N+1, \\ \gamma^n|g|^{2n}\binom{n-1}{N}^2 & \text{if } n > N+1. \end{cases} \quad (4)$$

For $n \le N+1$, $G^{(n)}_{\rm trans}(0)$ scales as $|g|^{2(N+1)}$, matching the probability density of simultaneously detecting $N+1$ photons from the drive. In contrast, for $n > N+1$, the $n$ th-order correlation function of both the transmitted field and input drive scale as $|g|^{2n}$. This scaling highlights that transmission is a process unlocked by at least $N+1$ input photons from the drive. While transmission events are rare in the weak driving regime, the second-order coherence function $g^{(2)}_{\rm trans}(0) = G^{(2)}_{\rm trans}(0)/[G^{(1)}_{\rm trans}(0)]^2 \propto |g|^{-2(N+1)} \gg 1$ reveals superbunched [49] transmission when it occurs. To further understand this $(N+1)$-photon transmission process, we next examine the atomic system's quantum state conditioned on transmission.

*Conditional atomic state*—When conditioning the steady state from Eq. (2) on detecting a transmitted photon, we obtain the maximally mixed state

$$\rho_c = \frac{a_{\text{out}}^R \rho a_{\text{out}}^{R\dagger}}{\langle a_{\text{out}}^{R\dagger} a_{\text{out}}^R \rangle} = \frac{I_{N+1}}{N+1}. \quad (5)$$

In the strong driving regime, $|g| \gg 1$, the conditional state in Eq. (5), to leading order, coincides with the steady state in Eq. (2), as the drive saturates the atomic system and photon detections have a negligible effect on the state. However, the conditional state in Eq. (5) is *independent* of the normalized drive amplitude $g$. This raises the question of how to understand this state in the weak driving regime, $|g| \ll 1$, where the steady state is close to the ground state. In this regime, while the probability of detecting a transmitted photon is small, proportional to $|g|^{2(N+1)}$, when such a photon is detected, Eq. (5) tells us that the atomic system has an average of $N/2$ excitations. This can be understood by highlighting the fact that we are conditioning on detecting *any* transmitted photon. Transmission occurs only in bunches, as seen from Eqs. (3) and (4), following the collective excitation of all atoms, and each photon in the bunch could have been emitted from any excitation level of the system. This lack of information about which excitation level the transmitted photon was emitted from leads to maximal uncertainty in the atomic state.

To determine the atomic state after a specific transmitted click, we turn to the normalized no-click master equation, a master equation with removed jump and click terms describing the system evolution between detection events [54,64–66]. In the weak driving regime, the photon scattering rate is small, justifying the study of the no-click master equation. First, we consider the evolution described in Eq. (1) without transmitted clicks by removing the term $a_{\text{out}}^R \rho a_{\text{out}}^{R\dagger}$. When we condition the steady state of this no-click evolution on an inevitable transmitted detection, we obtain the atomic state after the *first* transmitted click in a photon bunch. Using $|k\rangle_{\text{ex}}$ to denote the state with $k$ excited atoms, this first-click state is given by [54]

$$\rho_c^{\text{first}} = \sum_{k=0}^{N} \frac{1}{2^{N-k}(2-2^{-N})} |k\rangle\langle k|_{\text{ex}}. \quad (6)$$

Notably, the state in Eq. (6) follows an $N$-truncated geometric distribution, arising from the possibility of $N-k$ reflected photons preceding the first transmitted photon. This distribution is consistent with all incoherent scattering events involving $N+1$ photons, each having an equal $1/2$ probability of transmission or reflection. The highest probability corresponds to the fully excited state, i.e., $k = N$, occurring when the first photon is transmitted, and decreases by half with each additional previously reflected photon. The geometric distribution reveals that transmission originates from the fully excited state. We, thus, consider Eq. (1) without both reflected and transmitted clicks by removing the jump terms $a_{\text{out}}^L \rho a_{\text{out}}^{L\dagger}$ and $a_{\text{out}}^R \rho a_{\text{out}}^{R\dagger}$. Indeed, conditioning the steady state of this no-click evolution on an inevitable transmitted detection yields the fully excited atomic state $|N\rangle_{\text{ex}}$, confirming that transmission occurs through a process where all $N$ atoms are excited.

*Timescales*—Having established that transmission is a multiphoton process, enabled when $(N+1)$ or more photons scatter off the atoms, we now make this picture more quantitative by defining the timescale $T_{\text{in}}$ within which these photons must arrive to enable this transmission. In the weak-drive regime, transmission is dominated by the incoming rate of $N+1$ photons, as shown in Eq. (3). Incoming photons follow a Poisson distribution, and under weak driving, the probability of $N+1$ photons arriving within time $T_{\text{in}}$ is $(\gamma|g|^2 T_{\text{in}})^{N+1}/(N+1)!$. These incoming photons yield $(N+1)/2$ transmitted photons, as they can be either reflected or transmitted, resulting in an average transmission rate of $(\gamma|g|^2)^{N+1} T_{\text{in}}^N/(2N!)$ [54]. By equating this rate with the transmission rate from Eq. (3), we arrive at

$$T_{\text{in}} = \frac{1}{\gamma} \left( \frac{2(N+1)}{N!} \right)^{1/N}. \quad (7)$$

Equation (7) shows that, with increasing $N$, more input photons are required within a shorter time frame to trigger transmission. For large $N$, $T_{\text{in}}$ is lower bounded by $e/(\gamma N)$, qualitatively agreeing with the increasing collective coupling of the atomic system.

The second relevant timescale, $T_{\text{out}}$, characterizes the relaxation of an excited atomic state. From the fully excited state $|N\rangle_{\text{ex}}$, the atomic system undergoes cascaded emission from $|k\rangle_{\text{ex}}$ to $|k-1\rangle_{\text{ex}}$ at rates $\Gamma_k = 2\gamma\langle k|S_+S_-|k\rangle_{\text{ex}} = 2\gamma(N-k+1)k$ until reaching the ground state $|0\rangle_{\text{ex}}$. This process forms a continuous-time absorbing Markov chain with $N+1$ states, where decay times between adjacent states follow exponential distributions with rates $\Gamma_k$. The total relaxation time follows a hypoexponential distribution [67–69], which is the sum of independent exponential random variables, with rate parameters $\Gamma_N, \ldots, \Gamma_1$. Crucially, this statistical framework enables calculation of the $p$ th relaxation time quantile, $T_{\text{out},p}$, defined as the time by which the atomic system reaches the ground state with probability $p$. Additionally, the average relaxation time [5,54] is given by $T_{\text{out,avg}} = \sum_{k=1}^{N} (1/\Gamma_k) = [H_N/\gamma(N+1)]$, where $H_N$ is the $N$ th harmonic number. The asymptotic limit for large $N$ is $\ln(N)/(\gamma N)$, characteristic of superradiant collective spontaneous emission [5]. With these timescales established, we now turn to photon detection statistics obtained by numerical simulations.

*Photon detection statistics*—The master equation in Eq. (1) is simulated using Monte Carlo trajectory evolution [64,70], with the output operators $a_{\text{out}}^{R/L}$ corresponding to photon detection in the transmitted and reflected fields according to Fig. 1. Here, we present results for $N = 3$ atoms, while results for $N = 1$ and 2 atoms can be found in

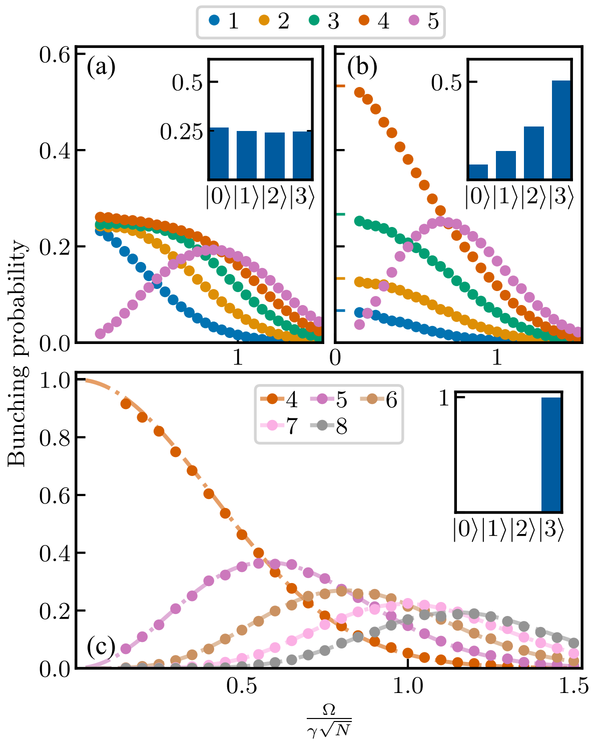


FIG. 2. Bunching probability versus effective drive amplitude $\Omega/(\gamma\sqrt{N})$, with $N = 3$ atoms, $\gamma = 1$, $T_{\mathrm{in}} = 1.10$ according to Eq. (7), and $T_{\mathrm{out}} = T_{\mathrm{out},99\%} = 1.30$. The circles show simulation results, and different colors represent different photon bunch sizes. The insets display the average atomic state populations, conditioned on the first transmitted click, for the simulations with the weakest drive strength. For stronger drive strengths, the probabilities sum to less than one as the curves for larger-sized bunches are omitted. (a) All transmitted photons are counted as first clicks; i.e., clicks are recounted. (b) The first transmitted click is defined as a transmitted detection preceded by no other transmitted photons during the time $T_{\mathrm{in}}$. (c) The first transmitted click is defined as a transmitted detection preceded by neither transmitted nor reflected photons during the time $T_{\mathrm{in}}$. The dash-dotted lines represent analytical predictions from Eq. (8) with the fitted timescales $\hat{T}_{\mathrm{in}} = 0.37$ and $\hat{T}_{\mathrm{out}} = 0.93$.

Fig. 4 in End Matter. For our analysis, a photon bunch is defined by the number of clicks in the reflected and transmitted fields within a bunching time $T_{\mathrm{out}}$ after, and including, the first transmitted click. Figure 2 shows the probability of obtaining a photon bunch of a given size versus the effective drive amplitude $\Omega/(\gamma\sqrt{N})$, demonstrating that different definitions of the *first transmitted click* yield different photon bunching statistics.

In Fig. 2(a), we employ a simple counting method where every transmitted photon is treated as a first click, effectively recounting photons that belong to the same bunching event. In the weak-drive regime, we detect the mixed state as predicted in Eq. (5); however, for larger drive strengths, most of the detected photons originate directly from the coherent drive and bunches typically contain more than five photons. In Fig. 2(b), we instead define the first transmitted click as a transmitted detection preceded by no other transmitted photons within the characteristic timescale $T_{\mathrm{in}}$. In the weak-drive regime, the bunching probabilities approach the truncated geometric distribution, as predicted in Eq. (6).

In Fig. 2(c), we define the first transmitted click as a transmitted detection preceded by neither transmitted nor reflected photons during the time $T_{\mathrm{in}}$. In the weak-drive regime, we approach exclusively $(N+1)$-photon bunches, as predicted by the no-click master equation. The analytical prediction for a $k$-photon bunch probability [54], plotted in Fig. 2(c), is given by

$$p(k) = \sum_{i=0}^{k-N-1} \Pr(Y = k-i)\,\Pr(Z = i), \tag{8}$$

where $k \geq N+1$. The random variable $Y$, representing the initial photons that trigger transmission, follows an $N$-truncated Poisson distribution, while $Z$, accounting for additional input photons arriving during the emission process, follows a Poisson distribution. The summation in Eq. (8) captures all possible combinations of initial and additional photons that result in a $k$-photon bunch. For example, an $(N+2)$-photon bunch arises from either $N+2$ initial photons with no additional arrivals or $N+1$ initial photons plus one additional arrival. The random variables $Y$ and $Z$ have the parameters $|\alpha|^2\hat{T}_{\mathrm{in}}$ and $|\alpha|^2\hat{T}_{\mathrm{out}}$, respectively, where the timescales $\hat{T}_{\mathrm{in}}$ and $\hat{T}_{\mathrm{out}}$ are obtained by fitting Eq. (8) to the simulation data. Interestingly, while these fitted timescales are systematically found to be shorter than those used to define photon bunches in the simulations [54], the analytical prediction of Eq. (8), nonetheless, shows excellent agreement with the numerical data in Fig. 2(c), even at intermediate and strong drive. In the weak driving regime, the probability of obtaining an $(N+1)$-photon bunch from Eq. (8) can be approximated by $p(N+1) = e^{-\Omega^2\hat{T}_{\mathrm{out}}/\gamma}$, which represents the heralding efficiency and shows an exponential convergence to $(N+1)$-photon bunches [54].

*Applications*—Naturally, our simple setup enables multiphoton state generation and entanglement distribution, heralded by the detection of the first transmitted photon. Specifically, the bidirectional spontaneous emission from fully excited atoms produces an entangled two-mode binomial state [71], $|\psi_{\mathrm{b}}\rangle = \sum_{k=0}^{N}\left[\binom{N}{k}2^{-N}\right]^{1/2}|k, N-k\rangle_{\mathrm{L,R}}$, between the left and right propagating modes. Figure 3 shows the fidelity $\langle\psi_{\mathrm{b}}|\varrho_{\mathrm{out}}|\psi_{\mathrm{b}}\rangle$ between the caught output state $\varrho_{\mathrm{out}}$ and the binomial state versus the effective drive amplitude $\Omega/(\gamma\sqrt{N})$ for up to eight atoms. Following [72,73], we catch the output state by filtering with the optimal output mode shape corresponding to fully excited atoms decaying without drive. As shown in Fig. 3, the fidelity decreases with increased drive amplitude, as atomic

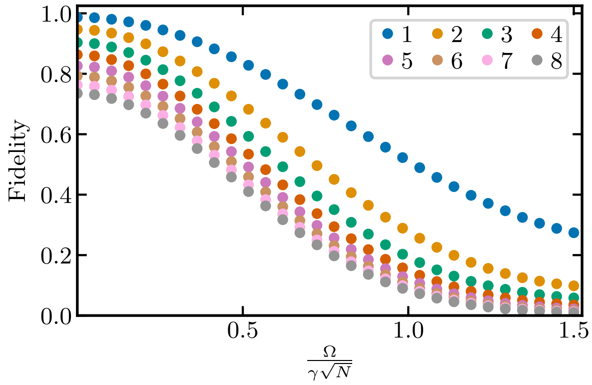


FIG. 3. Fidelity of the output field with the entangled binomial state, versus effective drive amplitude $\Omega/(\gamma\sqrt{N})$, for a system of initially fully excited atoms, with $N = 1$–8 atoms represented by different colored markers and $\gamma = 1$. The output states are taken at time $T_{\mathrm{out},99\%}$.

emission is superposed with the coherent drive. In the weak-drive regime of interest, however, the fidelity is essentially unchanged from the zero-drive case. Furthermore, lower fidelities correspond to higher atom numbers, as nonlinear decay generates multimode output states. Nevertheless, the optimal mode captures at least 90% of the output photons for up to eight atoms [8], and, if we capture all or multiple temporal modes, the fidelity in Fig. 3 would approach unity for the zero-drive case. Moreover, placing a mirror at an appropriate distance from the atoms in the transmitted direction [74] channels all $N$ photons to propagate in a single direction. This enables applications in quantum metrology for quantum-enhanced phase measurements [7–9] and quantum lithography to beat the diffraction limit [12,13].

*Discussion*—In summary, we have demonstrated that coherently driven atoms in a waveguide generate super-bunched light, with the first transmitted photon heralding the atoms in a fully excited state. In a wider scope, by applying the no-click master equation, we reveal the multiphoton emission mechanisms which enable a novel route to heralded multiphoton state generation. While we initially envision experimental setups with a few to tens of atoms, the validity of the Markov approximation on photon bunching for larger systems warrants future investigation. Additionally, we plan to study how imperfections in realistic setups like dephasing, detuning, anharmonicity in transmon systems, and detector inefficiencies affect photon bunching robustness.

*Acknowledgments*—We thank I. Lyngfelt and B. Bertin-Johannet for feedback on the manuscript. We acknowledge support from the Knut and Alice Wallenberg Foundation through the Wallenberg Centre for Quantum Technology (WACQT). Z. Z. and G. J. acknowledge support from the Swedish Research Council, Grant No. 2021-04037. T. K. acknowledges support from the FY2024 JSPS Postdoctoral Fellowship for Research in Japan. The simulations were enabled by resources provided by the National Academic Infrastructure for Supercomputing in Sweden (NAISS), partially funded by the Swedish Research Council through Grant No. 2022-06725.

*Data availability*—The data that support the findings of this article are not publicly available. The data are available from the authors upon reasonable request.


[1] N. V. Corzo, J. Raskop, A. Chandra, A. S. Sheremet, B. Gouraud, and J. Laurat, Nature (London) **566**, 359 (2019).
[2] A. S. Sheremet, M. I. Petrov, I. V. Iorsh, A. V. Poshakinskiy, and A. N. Poddubny, Rev. Mod. Phys. **95**, 015002 (2023).
[3] A. S. Prasad, J. Hinney, S. Mahmoodian, K. Hammerer, S. Rind, P. Schneeweiss, A. S. Sørensen, J. Volz, and A. Rauschenbeutel, Nat. Photonics **14**, 719 (2020).
[4] R. H. Dicke, Phys. Rev. **93**, 99 (1954).
[5] M. Gross and S. Haroche, Phys. Rep. **93**, 301 (1982).
[6] A. Goban, C.-L. Hung, J. D. Hood, S.-P. Yu, J. A. Muniz, O. Painter, and H. J. Kimble, Phys. Rev. Lett. **115**, 063601 (2015).
[7] V. Paulisch, M. Perarnau-Llobet, A. González-Tudela, and J. I. Cirac, Phys. Rev. A **99**, 043807 (2019).
[8] M. Perarnau-Llobet, A. González-Tudela, and J. I. Cirac, Quantum Sci. Technol. **5**, 025003 (2020).
[9] M. Khanahmadi and K. Mølmer, Phys. Rev. A **107**, 013705 (2023).
[10] B. Blauensteiner, I. Herbauts, S. Bettelli, A. Poppe, and H. Hübel, Phys. Rev. A **79**, 063846 (2009).
[11] M. Maffei, D. Pomarico, P. Facchi, G. Magnifico, S. Pascazio, and F. V. Pepe, Phys. Rev. Res. **6**, L032017 (2024).
[12] A. N. Boto, P. Kok, D. S. Abrams, S. L. Braunstein, C. P. Williams, and J. P. Dowling, Phys. Rev. Lett. **85**, 2733 (2000).
[13] G. Björk, L. L. Sánchez-Soto, and J. Söderholm, Phys. Rev. Lett. **86**, 4516 (2001).
[14] D. E. Chang, A. S. Sørensen, E. A. Demler, and M. D. Lukin, Nat. Phys. **3**, 807 (2007).
[15] E. Vetsch, D. Reitz, G. Sagué, R. Schmidt, S. T. Dawkins, and A. Rauschenbeutel, Phys. Rev. Lett. **104**, 203603 (2010).
[16] A. Goban, K. S. Choi, D. J. Alton, D. Ding, C. Lacroûte, M. Pototschnig, T. Thiele, N. P. Stern, and H. J. Kimble, Phys. Rev. Lett. **109**, 033603 (2012).
[17] A. Goban, C.-L. Hung, S.-P. Yu, J. Hood, J. Muniz, J. Lee, M. Martin, A. McClung, K. Choi, D. Chang, O. Painter, and H. Kimble, Nat. Commun. **5**, 3808 (2014).
[18] J. D. Hood, A. Goban, A. Asenjo-Garcia, M. Lu, S.-P. Yu, D. E. Chang, and H. J. Kimble, Proc. Natl. Acad. Sci. U.S.A. **113**, 10507 (2016).
[19] N. V. Corzo, B. Gouraud, A. Chandra, A. Goban, A. S. Sheremet, D. V. Kupriyanov, and J. Laurat, Phys. Rev. Lett. **117**, 133603 (2016).
[20] H. L. Sørensen, J.-B. Béguin, K. W. Kluge, I. Iakoupov, A. S. Sørensen, J. H. Müller, E. S. Polzik, and J. Appel, Phys. Rev. Lett. **117**, 133604 (2016).
[21] P. Solano, P. Barberis-Blostein, F. K. Fatemi, L. A. Orozco, and S. L. Rolston, Nat. Commun. **8**, 1857 (2017).

[22] R. Pennetta, M. Blaha, A. Johnson, D. Lechner, P. Schneeweiss, J. Volz, and A. Rauschenbeutel, Phys. Rev. Lett. **128**, 073601 (2022).

[23] P. Lodahl, A. Floris van Driel, I. S. Nikolaev, A. Irman, K. Overgaag, D. Vanmaekelbergh, and W. L. Vos, Nature (London) **430**, 654 (2004).

[24] O. Astafiev, A. M. Zagoskin, A. A. Abdumalikov, Y. A. Pashkin, T. Yamamoto, K. Inomata, Y. Nakamura, and J. S. Tsai, Science **327**, 840 (2010).

[25] A. A. Abdumalikov, O. Astafiev, A. M. Zagoskin, Y. A. Pashkin, Y. Nakamura, and J. S. Tsai, Phys. Rev. Lett. **104**, 193601 (2010).

[26] I.-C. Hoi, C. M. Wilson, G. Johansson, T. Palomaki, B. Peropadre, and P. Delsing, Phys. Rev. Lett. **107**, 073601 (2011).

[27] I.-C. Hoi, T. Palomaki, J. Lindkvist, G. Johansson, P. Delsing, and C. M. Wilson, Phys. Rev. Lett. **108**, 263601 (2012).

[28] K. Lalumière, B. C. Sanders, A. F. van Loo, A. Fedorov, A. Wallraff, and A. Blais, Phys. Rev. A **88**, 043806 (2013).

[29] I.-C. Hoi, C. M. Wilson, G. Johansson, J. Lindkvist, B. Peropadre, T. Palomaki, and P. Delsing, New J. Phys. **15**, 025011 (2013).

[30] A. F. van Loo, A. Fedorov, K. Lalumière, B. C. Sanders, A. Blais, and A. Wallraff, Science **342**, 1494 (2013).

[31] B. Peropadre, J. Lindkvist, I.-C. Hoi, C. M. Wilson, J. J. Garcia-Ripoll, P. Delsing, and G. Johansson, New J. Phys. **15**, 035009 (2013).

[32] J.-L. Orgiazzi, C. Deng, D. Layden, R. Marchildon, F. Kitapli, F. Shen, M. Bal, F. R. Ong, and A. Lupascu, Phys. Rev. B **93**, 104518 (2016).

[33] F. Yan, S. Gustavsson, A. Kamal, J. Birenbaum, A. P. Sears, D. Hover, T. J. Gudmundsen, D. Rosenberg, G. Samach, S. Weber, J. L. Yoder, T. P. Orlando, J. Clarke, A. J. Kerman, and W. D. Oliver, Nat. Commun. **7**, 12964 (2016).

[34] M. Mirhosseini, E. Kim, X. Zhang, A. Sipahigil, P. B. Dieterle, A. J. Keller, A. Asenjo-Garcia, D. E. Chang, and O. Painter, Nature (London) **569**, 692 (2019).

[35] J. D. Brehm, R. Gebauer, A. Stehli, A. N. Poddubny, O. Sander, H. Rotzinger, and A. V. Ustinov, Appl. Phys. Lett. **121**, 204001 (2022).

[36] M. Zanner, T. Orell, C. M. F. Schneider, R. Albert, S. Oleschko, M. L. Juan, M. Silveri, and G. Kirchmair, Nat. Phys. **18**, 538 (2022).

[37] E. S. Redchenko, M. Zens, M. Žemlička, M. Peruzzo, F. Hassani, R. Sett, P. Zieliński, H. S. Dhar, D. O. Krimer, S. Rotter, and J. M. Fink, Phys. Rev. Lett. **134**, 063601 (2025).

[38] J.-H. Kim, S. Aghaeimeibodi, C. J. K. Richardson, R. P. Leavitt, and E. Waks, Nano Lett. **18**, 4734 (2018).

[39] X. Luan, J. Béguin, A. P. Burgers, Z. Qin, S. Yu, and H. J. Kimble, Adv. Quantum Technol. **3**, 2000008 (2020).

[40] J. D. Brehm, A. N. Poddubny, A. Stehli, T. Wolz, H. Rotzinger, and A. V. Ustinov, npj Quantum Mater. **6**, 10 (2021).

[41] C. Papon, Y. Wang, R. Uppu, S. Scholz, A. D. Wieck, A. Ludwig, P. Lodahl, and L. Midolo, Phys. Rev. Appl. **19**, L061003 (2023).

[42] X.-L. Chu, C. Papon, N. Bart, A. D. Wieck, A. Ludwig, L. Midolo, N. Rotenberg, and P. Lodahl, Phys. Rev. Lett. **131**, 033606 (2023).

[43] A. Tiranov, V. Angelopoulou, C. J. van Diepen, B. Schrinski, O. A. D. Sandberg, Y. Wang, L. Midolo, S. Scholz, A. D. Wieck, A. Ludwig, A. S. Sørensen, and P. Lodahl, Science **379**, 389 (2023).

[44] X. Zhou, H. Tamura, T.-H. Chang, and C.-L. Hung, Phys. Rev. X **14**, 031004 (2024).

[45] A. Bouscal, M. Kemiche, S. Mahapatra, N. Fayard, J. Berroir, T. Ray, J.-J. Greffet, F. Raineri, A. Levenson, K. Bencheikh, C. Sauvan, A. Urvoy, and J. Laurat, New J. Phys. **26**, 023026 (2024).

[46] H. S. Han, A. Lee, S. Subhankar, F. K. Fatemi, and S. L. Rolston, arXiv:2509.22958.

[47] Z. Niu, W. Nie, D. Bao, X. He, W. Gao, K. Liu, I. C. Hoi, Y.-x. Liu, X. Xie, Z. Wang, and Z.-R. Lin, arXiv:2507.00935.

[48] D. Hallett, J. Wiercinski, L. Hallacy, S. Sheldon, R. Dost, N. Martin, A. Fenzl, I. Farrer, A. Verma, M. Cygorek, E. M. Gauger, M. S. Skolnick, and L. R. Wilson, Phys. Rev. Appl. **25**, L021003 (2026).

[49] Z. Ficek and S. Swain, *Quantum Interference and Coherence* (Springer-Verlag, Berlin, 2005).

[50] J. T. Shen and S. Fan, Opt. Lett. **30**, 2001 (2005).

[51] J.-T. Shen and S. Fan, Phys. Rev. Lett. **95**, 213001 (2005).

[52] H. Zheng, D. J. Gauthier, and H. U. Baranger, Phys. Rev. A **82**, 063816 (2010).

[53] Xin H. H. Zhang and H. U. Baranger, Phys. Rev. A **97**, 023813 (2018).

[54] See Supplemental Material at http://link.aps.org/supplemental/10.1103/6fcg-2zns for lengthier derivations, which includes Refs. [55,56].

[55] J. Riordan, *Combinatorial Identities*, Wiley Series in Probability and Mathematical Statistics (John Wiley & Sons, Nashville, TN, 1968), 99th ed.

[56] M. Mitzenmacher and E. Upfal, *Probability and Computing: Randomized Algorithms and Probabilistic Analysis* (Cambridge University Press, Cambridge, England, 2005).

[57] R. R. Puri and S. V. Lawande, Phys. Lett. **72A**, 200 (1979).

[58] R. Puri and S. Lawande, Physica (Amsterdam) **101A**, 599 (1980).

[59] P. D. Drummond, Phys. Rev. A **22**, 1179 (1980).

[60] S. V. Lawande, R. R. Puri, and S. S. Hassan, J. Phys. B **14**, 4171 (1981).

[61] S. Hassan, R. Bullough, R. Puri, and S. Lawande, Physica (Amsterdam) **103A**, 213 (1980).

[62] S. S. Hassan, G. P. Hildred, R. R. Puri, and R. K. Bullough, J. Phys. B. **15**, 2635 (1982).

[63] R. J. Glauber, Phys. Rev. **130**, 2529 (1963).

[64] K. Mølmer, Y. Castin, and J. Dalibard, J. Opt. Soc. Am. B **10**, 524 (1993).

[65] H.-P. Breuer and F. Petruccione, *The Theory of Open Quantum Systems* (Oxford University Press, New York, 2007).

[66] H. M. Wiseman and G. J. Milburn, *Quantum Measurement and Control* (Cambridge University Press, Cambridge, England, 2009).

[67] S. Amari and R. Misra, IEEE Trans. Reliab. **46**, 519 (1997).

[68] G. Bolch, S. Greiner, H. de Meer, and K. S. Trivedi, *Queueing Networks and Markov Chains: Modeling and Performance Evaluation with Computer Science Applications* (Wiley, New York, 2006).

[69] B. Legros and O. Jouini, Appl. Math. Model. **39**, 4971 (2015).

[70] N. Lambert, E. Giguère, P. Menczel, B. Li, P. Hopf, G. Suárez, M. Gali, J. Lishman, R. Gadhvi, R. Agarwal, A. Galicia, N. Shammah, P. Nation, J. R. Johansson, S. Ahmed, S. Cross, A. Pitchford, and F. Nori, Phys. Rep. **1153**, 1 (2026).

[71] S. R. Miry, M. K. Tavassoly, and R. Roknizadeh, J. Opt. Soc. Am. B **31**, 270 (2014).

[72] A. H. Kiilerich and K. Mølmer, Phys. Rev. Lett. **123**, 123604 (2019).

[73] M. Khanahmadi, M. M. Lund, K. Mølmer, and G. Johansson, Phys. Rev. Res. **5**, 043071 (2023).

[74] S. R. Sathyamoorthy, A. Bengtsson, S. Bens, M. Simoen, P. Delsing, and G. Johansson, Phys. Rev. A **93**, 063823 (2016).


## End Matter

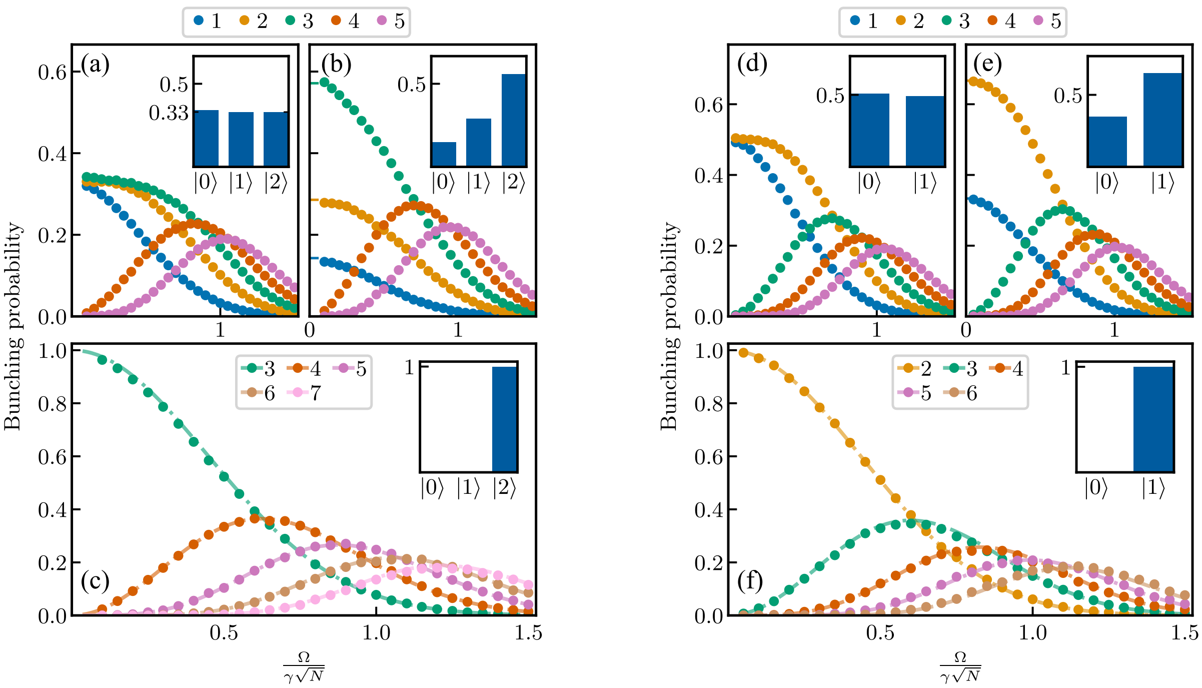


FIG. 4. Bunching probability versus effective drive amplitude $\Omega/(\gamma\sqrt{N})$. The left (right) panel corresponds to $N = 2(1)$ atoms, with the simulation parameters $\gamma = 1$, $T_{\mathrm{in}} = 1.70$, $T_{\mathrm{out}} = T_{\mathrm{out},99\%} = 1.66$ and $\gamma = 1$, $T_{\mathrm{in}} = 4$, $T_{\mathrm{out}} = T_{\mathrm{out},99.9\%} = 3.45$, respectively. The circles show simulation results, and different colors represent different photon bunch sizes. The insets display the average atomic state populations, conditioned on the first transmitted click, for the simulations with the weakest drive strength. For stronger drive strengths, the probabilities sum to less than one as the curves for larger-sized bunches are omitted. (a),(d) All transmitted photons are counted as first clicks; i.e., clicks are recounted. (b),(e) The first transmitted click is defined as a transmitted detection preceded by no other transmitted photons during the time $T_{\mathrm{in}}$. (c),(f) The first transmitted click is defined as a transmitted detection preceded by neither transmitted nor reflected photons during the time $T_{\mathrm{in}}$. The dash-dotted lines represent analytical predictions from Eq. (8) with the fitted timescales $\hat{T}_{\mathrm{in}} = 0.83$ and $\hat{T}_{\mathrm{out}} = 1.05$ for the left panel and $\hat{T}_{\mathrm{in}} = 2.58$ and $\hat{T}_{\mathrm{out}} = 1.80$ for the right panel.